Accepted Manuscript

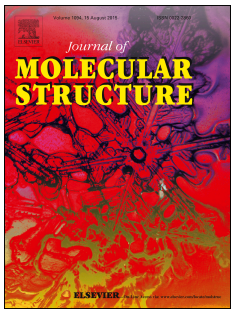

Spectroscopic characterization, antimicrobial activity and molecular docking study of novel azo-imine functionalized sulphamethoxazoles

Nilima Sahu, Sudipa Mondal, Kaushik Naskar, Ananya Das Mahapatra, Suvroma Gupta, Alexandra M.Z. Slawin, Debprasad Chattopadhyay, Chittaranjan Sinha

PII: S0022-2860(17)31371-6

DOI: 10.1016/j.molstruc.2017.10.040

Reference: MOLSTR 24411

To appear in: *Journal of Molecular Structure*

Received Date: 26 July 2017

Revised Date: 11 October 2017

Accepted Date: 11 October 2017

Please cite this article as: N. Sahu, S. Mondal, K. Naskar, A.D. Mahapatra, S. Gupta, A.M.Z. Slawin, D. Chattopadhyay, C. Sinha, Spectroscopic characterization, antimicrobial activity and molecular docking study of novel azo-imine functionalized sulphamethoxazoles, *Journal of Molecular Structure* (2017), doi: 10.1016/j.molstruc.2017.10.040.

Spectroscopic characterization, antimicrobial activity and Molecular Docking Study of novel azo-imine functionalized sulphamethoxazoles

Nilima Sahu, Sudipa Mondal , Kaushik Naskar, Anyna Das Mahapatra, Suvroma Gupta, Alexandra M. Z. Slawin , Debprasad Chattopadhyay and Chittaranjan Sinha*

Sulfamethoxazolyl-azo-imine derivatives (**1**, **2a-f**) have been examined against gram positive bacteria, *B. subtillis* and gram negative *E. coli* and have found effective selectively on *B. subtillis*. Some of them also show antiviral activity against HSV-1Finfection. The structures of the compounds are supported by different spectroscopic data and single crystal X-ray structure of **2c**. The compounds have been docked in the DHPS protein cavity to examine their binding strength and **2c** shows highest binding strength.

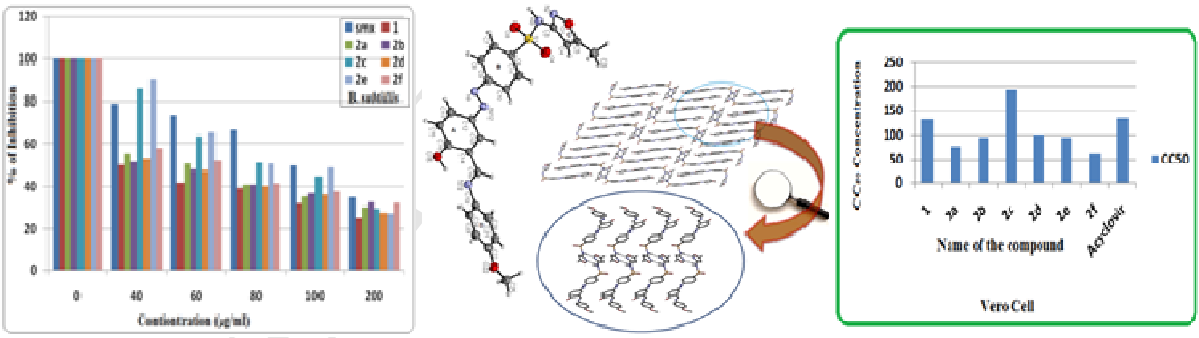

Spectroscopic characterization, antimicrobial activity and Molecular Docking Study of novel azo-imine functionalized sulphamethoxazoles

Nilima Sahu[a,1], Sudipa Mondal[a] , Kaushik Naskar[a], Ananya Das Mahapatra[b], Suvroma Gupta[c], Alexandra M. Z. Slawin[d] , Debprasad Chattopadhyay[b] and Chittaranjan Sinha[*a]

*Address for correspondence: c_r_sinha@yahoo.com (C. Sinha); fax-+91-2414-6584

[a]Department of Chemistry, Jadavpur University, Kolkata-700032, West Bengal, India

[b]ICMR Virus Unit, Infectious Diseases & Beliaghata General Hospital, GB-4, 57, S. C. Bannerjee Road, Beliaghata, Kolkata – 700 010, West Bengal, India

[c]Department of Biotechnology, Haldia Institute of Technology, Haldia, Purba Medinipur, West Bengal, Pin – 721657, India

[d]Molecular Structure Laboratory, School of Chemistry, University of St. Andrews, Purdie Building, St. Andrews, Fife, KY16 9ST, UK

Abstract

[SMX-N=N-C_6H_3-(*p*-OH)(*m*-CHO)] (**1**) reacts with $ArNH_2$ to synthesize Schiff bases, [SMX-N=N-C_6H_3-(*p*-OH)(*m*-HC=N-Ar)] (Ar = $–C_6H_5$ (**2a**), $–C_6H_4$-*p*-CH_3 (**2b**), $–C_6H_4$-*p*-OCH_3 (**2c**), $–C_6H_4$-*p*-*Cl* (**2d**), $–C_6H_4$-*p*-NO_2 (**2e**), $–C_{10}H_7$ (**2f**)) and the products have been assessed for antibacterial properties against Gram positive bacteria, *B. subtillis* : IC_{50} (μg/ml) : 39.2 (**1**), 60.1 (**2a**), 64.0 (**2b**), 85.6 (**2c**), 55.1 (**2d**), 88.4 (**2e**) and 65.1 (**2f**); and Gram negative bacteria, *E. coli*: IC_{50} (μg/ml) : 159.0 (**1**), 151.4 (**2a**), 155.3 (**2b**), 140 (**2c**), 156.0 (**2d**), 153.5 (**2e**) and 157 (**2f**). The cell line toxicity (Vero cells) has also been evaluated with these compounds and EC_{50} (μg/ml) values are 129.9 (**1**), 74.2 (**2a**) and 93.0 (**2b**), 191.9 (**2c**), 99.1 (**2d**), 93.2 (**2e**) and 62.0

(**2f**). The anti-viral efficiency against harpies virus (HSV-1F ATCC-733) infection demonstrates that the compound **1** has highest selectivity index (CC_{50}/EC_{50}), 5.06 than the compounds **2a-f** (CC_{50}/EC_{50} : 1.18 (**2a**), 1.42 (**2b**), 3.50 (**2c**), 1.45 (**2d**), 1.58 (**2e**), 1.29 (**2f**)). The compounds have been spectroscopically characterized and the structural confirmation has been established in one case by single crystal X-ray diffraction studies of **2c**. *In silico* Molecular Docking study has been done using optimized geometries of the compounds to search the most favored binding mode of these drugs and hence useful to explain their competitive drug efficiency.

Keywords: Schiff base of SMX-N=N-salicylaldehyde, X-ray structure, antimicrobial activity, cell line toxicity, molecular docking, DFT.

1. Introduction

Dr. Paul Ehrlich synthesized arsphenamine (known as salvarsan) in 1907 and used as antisyphilitic drug since 1909 [1]. Dr. Paul discovered an azo dye, Prontosil, in 1932 which resembles the structure to salvarsan and used as less toxic more efficient drug against syphilis [2]. It has been noticed that in the human body prontosil is converted to sulphanilamide which is the real active compound. Thus the sulfa drugs or Sulfonamides were discovered. Since 1968, clinical use of the antibiotic has dramatically increased.

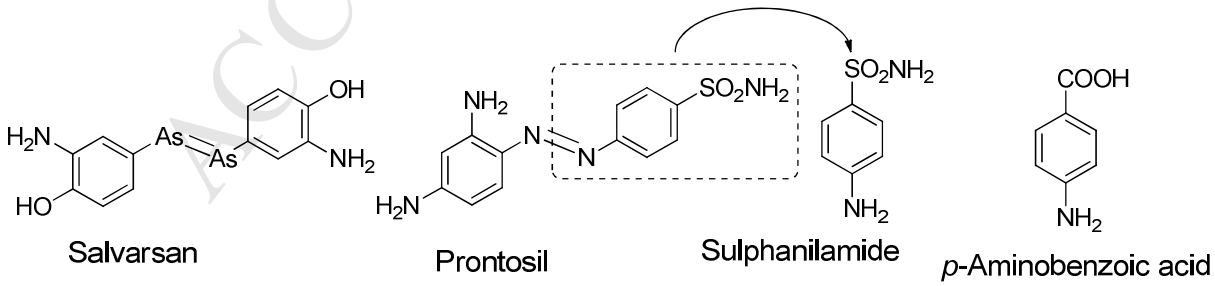

Sulfonamides inhibit DHPS (dihydropteroate synthetase) in the catalytic participation of the condensation of *p*-aminobenzoic acid (PABA) with 6-hydroxymethyl-dihydropterin

diphosphate (DHPS) due to its analogous structure [3]. Sulfamethoxazole (SMX), a common antibacterial agent against gram positive and gram negative bacteria, is most often used as part of the synergistic combination with trimethoprim in a 5:1 ratio in co-trimoxazole [4]. Prolong administration of SMX may cause toxicity like gastrointestinal upset, skin rashes, breathing trouble, add to the kidney damage and stomach or abdomen pain, nausea, headache [5-8]. The hypersensitivity arises due to oxidative metabolite such as SMX-hydroxylamine (SMX-NHOH) and SMX-nitroso (SMX-NO) [9]. In search of more effective and low toxic drugs the chemical and biological modification of antibiotics has taken tremendous momentum in the area of synthetic and pharmaceutical chemistry [10]. Azo compounds show a variety of interesting biological activities such as, anti-neoplastics, anti-diabetics, anti-septics, anti-HIV and other useful chemotherapeutic properties [11]. During last couple of years we have designed some sulfonamide derivatives incorporating imine (-C=N-) [12, 13] and azo (-N=N-) [14, 15] functions and the compounds have been used to investigate their antimicrobial activity. In this work, we have characterized hitherto unknown azo-imine (-N=N-C=N-) functionalized sulfamethoxazole (**Scheme 1**) and their antibacterial and antiviral activity have been examined. Out of various functional groups the azo-imine function is π-acidic and monitors the electrochemical potential of the molecules [16]. The drug activity and toxicity of the compounds have been scrutinized in this work and the molecular docking studies have been adopted with DHPS protein (obtained from PDB source) and DNA to examine their binding at best pose condition of the compounds.

2. Experiment

2.1. Materials and methods

Sulfamethoxazole was purchased from Hi-Media. Sodium nitrite, sodium hydroxide, were available from S.D. Fine Chem. Ltd. Salicylaldehyde, aniline, *p*-toluidine, *p*-anisidine, *p*-chloroaniline, *p*-nitroaniline and α-naphthylamine were purchased from Sigma-Aldrich. Other chemicals and solvents of Analytical grade were obtained from Merck. The solvent was purified by standard procedure [17].

Microanalytical data (C, H, and N) were collected on Perkin–Elmer 2400 CHNS/O elemental analyzer. Spectroscopic data were obtained using the following instruments: UV–Vis spectra by Perkin–Elmer UV–Vis spectrophotometer model Lambda 25; FTIR spectra (KBr disk, 4000–400 cm^{-1}) by Perkin–Elmer FT-IR spectrophotometer model RX-1; the ^{1}H NMR spectra by Bruker (AC) 300/500 MHz FTNMR spectrometer. ESI mass spectra were recorded on a micro mass Q-TOF mass spectrometer (serial no. YA 263).

2.2. Synthesis of azo/imine functionalized sulfonamides

2.2a.4-(3-Formyl-4-hydroxy-phenylazo)-N-(5-methyl-isoxazol-3-yl)-benzenesulfonamide (1)

The sulfamethoxazolyl diazonium (SMX-N=N-$^{+}$) ion was prepared by dropwise addition of ice cold aqueous solution of sodium nitrite (0.136 g, 1.97 mmol) to HCl solution (3N, 18 ml) of sulfamethoxazole (0.5 g, 1.97 mmol) for 30 min. SMX-N=N-$^{+}Cl^{-}$ so formed was added to the ice cold sodium hydroxide (2.4 g) solution of salicylaldehyde (0.20 ml, 1.97 mmol) with continuous stirring and pH 7 was maintained to settle yellow precipitate. It was filtered and dried. The product was crystallized from aqueous methanol solution; purity was checked by TLC and purified by column chromatography (silica gel, 60-120 mesh) and the desired product was obtained with (1/10 v/v, CH_3CN/toluene) eluent. The yield of **1** was 60%.

Microanalytical data, SMX-N=N-C_6H_3(*p*-OH)(*m*-CHO), **1;** Mp. 223(2)°C ($C_{17}H_{14}N_4O_5S$) : Calcd. C, 52.84; H, 3.62 ; N, 14.50; Found C, 52.78; H, 3.70 ; N, 14.61%. Mass (m/z), $(M+H)^+$, 387.07 (**Supplementary Materials, Fig. S1**). FT-IR spectrum, ν_{max} (cm^{-1}) : 1084, ν(C-O); 1476, ν(N=N); 1659, ν(C=O); 1618, ν(C-N); 3345, ν(O-H); 1170, ν(S-O) (**Supplementary Materials, Fig. S2**). ^{1}H NMR spectrum, ($CDCl_3$) δ(17-CH_3)(oxazole), 2.38 (s); δ(O-H), 11.43 (s); δ(N-H), 6.26 (s) , δ(CHO) 10.04 (s); δ(4-H), 7.12 (d, J = 9.21 Hz); δ(7-H), 7.25 (s); δ(5-H), 8.20 (d, J = 8.22 Hz), δ(10,12-H), 7.98 (m); δ(9,13-H), 8.02(m); δ(16-H), 8.17 (s) ppm (**Supplementary Materials, Fig. S3**).

2.2b. Azo sulfonamide Schiff bases, SMX-N=N-C_6H_3(*p*-OH)(*m*-CH=N-Ar), (Ar = – C_6H_5 (2a), – C_6H_4 –*p*-CH_3 (2b), – C_6H_4 –*p*-OCH_3 (2c),– C_6H_4 -*p*-*Cl* (2d), – C_6H_4 –*p*-NO_2 (2e), -$C_{10}H_7$ (2f))

The hot methanol solution of **1** (0.1 g, 0.26 mmol) was refluxed with 1:1 molar ratio (0.30 mmol) of aromatic Ar-NH_2 (0.30 mmol) (Ar = – C_6H_5 (**2a**), – C_6H_4 –*p*-CH_3 (**2b**), – C_6H_4 –*p*-OCH_3 (**2c**),– C_6H_4-*p*-Cl (**2d**),– C_6H_4 –*p*-NO_2 (**2e**), -$C_{10}H_7$ (**2f**)) for 10 to 24 h. The solution was then allowed to evaporate slowly in air and orange yellow crystals were deposited on glass wall. The crystals were collected and TLC test was performed to check purity. The product was recrystallized from methanol solution. The yield was 55-75 %.

Microanalytical data, SMX-N=N-C_6H_3(*p*-OH)(*m*-CH=N-C_6H_5), $C_{23}H_{19}N_5O_4S$ (**2a**) (yield, 68%), Mp. 232°C ($C_{23}H_{19}N_5O_4S$) : Calcd. C, 59.86; H, 4.15 ; N, 15.18; Found C, 59.78; H, 4.19; N, 15.30%. Mass (m/z), $(M+H)^+$ (462.2) (**Supplementary Materials, Fig. S4**). FT-IR spectrum, ν_{max} (cm^{-1}) : 1101, ν(C-O); 1472, ν(N=N); 1618, ν(C=N); 3450, ν(O-H); 1174, ν(SO_2) (**Supplementary Materials, Fig. S5**);); ^{1}H NMR spectrum ($CDCl_3$) δ(17-CH_3)(oxazole) 2.38

(s); δ(16-H), 8.07 (s); δ(O-H), 14.10 (s); δ(N-H), 6.26 (s); δ(CH-N) 8.75 (s); δ(7-H), 8.07 (s); δ(5-H), 7.97(s); δ(4-H), 7.16 (d, J = 8.85 Hz); δ(10,12-H), 7.26 (m); δ(9,13-H), 7.31 (m); δ(20-24-H), 7.44(m) ppm (**Supplementary Materials, Fig. S6)**

SMX-N=N-C_6H_3(*p*-OH)(*m*-CH=N-C_6H_4-*p*-CH_3), $C_{24}H_{21}N_5O_4S$ (**2b**) (yield, 65%),**:** Mp. 247°C: Calcd. C, 60.62; H, 4.45; N, 14.73; Found C, 60.56; H, 4.40; N, 14.77 %. Mass (m/z), $(M+H)^+$(476.15) (**Supplementary Materials, Fig. S7**). FT-IR spectrum, ν_{max} (cm^{-1}):1091, ν(C-O); 1472, ν(N=N); 1618, ν(C=N); 3390, ν(O-H); 1174, ν(S-O) (**Supplementary Materials, Fig. S8**). ^{1}H NMR spectrum (DMSO-D_6) δ(17-CH_3)(oxazole), 2.29 (s); δ(16-H), 8.31 (s); (22-CH_3), 2.33 (s); δ(O-H), 10.21 (s); δ(N-H), 6.16 (s); δ(CH-N), 9.16 (s); δ(4-H), 7.15 (d, J = 8.9 Hz); δ(5-H), 7.30 (d, J = 7.97 Hz); δ(10,12-H), 7.41 (m); δ(9,13-H), 7.38 (m); δ(16-H), 8.31 (s); δ(4-H of phenyl) and 8.02 (s); δ(20-24-H), 7.30 ppm (m) (**Supplementary Materials, Fig. S9).**

SMX-N=N-C_6H_3(*p*-OH)(*m*-CH=N-C_6H_4-*p*-OCH_3), $C_{24}H_{21}N_5O_5S$ (**2c**) (yield, 73%),: Mp. 235°C: Calcd. C, 58.65; H, 4.31 ; N, 14.25; Found C, 58.58; H, 4.26; N, 14.18%. Mass (m/z), $(M+H)^+$(492.2) (**Supplementary Materials, Fig. S10**). FT-IR spectrum, ν_{max} (cm^{-1}) : 1091, ν(C-O); 1489, ν(N=N); 1616, ν(C=N); 3378, ν(O-H); 1174, ν(S-O) (**Supplementary Materials, Fig. S11**). ^{1}H NMR spectrum (DMSO-d_6) δ(17-CH_3)(oxazole), 2.22 (s); (22-O-CH_3-phenyl), 2.48 (s); δ(16-H), 8.29 (s); δ(O-H), 11.40 (s); δ(N-H), 6.15 (s); δ(CH-N) 9.15 (s); δ(4-H), 7.03 (d, J = 5.65 Hz); δ(5-H), 7.11 (d, J = 8.76 Hz); δ(7-H), 7.14 (s); δ(9,13-H), 7.51 (m); δ(10,12-H) 8.02 (m); δ(20, 24-H), 7.42 (m); δ(21,23-H), 7.17 (m) ppm (**Supplementary Materials, Fig. S-12).**

SMX-N=N-C_6H_3(*p*-OH)(*m*-CH=N-C_6H_4-*p*-Cl), $C_{23}H_{18}N_5O_4ClS$ (**2d**) (yield, 74%),**:** Mp. 238°C Calcd. C, 55.70; H, 3.66; N, 14.12; Found C, 55.63; H, 3.60; N, 14.21%. Mass (m/z), $(M+H)^{+,}$ (496.8) (**Supplementary Materials, Fig. S13**). FT-IR spectrum, ν_{max} (cm^{-1}) :1093, ν(C-O); 1505, ν(N=N); 1621, ν(C-N); 3443, ν (O-H); 1180, ν(S-O) (**Supplementary Materials, Fig. S14**). ^{1}H

NMR spectrum (DMSO-d_6) δ(17-CH_3)(oxazole) 2.28 (s); δ(16-H), 8.35 (s); δ(O-H), 13.80 (s); δ(N-H), 6.16 (s); δ(CH-N) 9.15 (s); δ(4-H), 7.19 (d, J = 8.94 Hz); δ(5-H), 7.50 (m); δ(9,13-H), 7.47 (m); δ(10,12-H) 7.98 (s); δ(21,23-H), 7.15 (m); δ(7-H), 8.35 (s); δ(20,24-H), 7.45 (m) ppm (**Supplementary Materials, Fig. S-15**).

SMX-N=N-C_6H_3(*p*-OH)(*m*-CH=N-C_6H_4-*p*-NO_2), $C_{23}H_{18}N_6O_6S$ (**2e**) (yield, 55%),**:** Mp. 185°C: Calcd. C, 54.54; H, 3.58; N, 16.59; Found C, 54.48; H, 3.66; N, 16.68%. Mass (m/z), $(M+H)^+$ (507.5) (**Supplementary Materials, Fig. S16**). FT-IR spectrum, ν_{max} (cm^{-1}): 1099, ν(C-O); 1473, ν(N=N); 1613, ν(C-N); 3393, ν(O-H); 1174, ν(S-O) (**Supplementary Materials, Fig. S17**). ^1H NMR spectrum (DMSO-d_6) δ(17-CH_3)(oxazole), 2.37(s); δ(16-H), 8.26 (s); δ(O-H), 11.42 (s); δ(N-H), 6.25 (s); δ(CH-N) 10.03 (s); δ(4-H), 7.43 (d, J = 8.13 Hz); δ(5-H), 7.80 (d, J = 8.07 Hz); δ(7-H), 7.86 (s); δ(10,12-H), 7.12 (m); δ(9,13-H), 7.41 (m); δ(20, 24-H), 7.57 (m); δ(21,23-H), 8.02 (m) ppm (**Supplementary Materials, Fig. S18).**

SMX-N=N-C_6H_3(*p*-OH)(*m*-CH=N-(α)-$C_{10}H_7$), $C_{27}H_{21}N_5O_4S$, (**2f**) (yield, 64%), Mp. 130°C Calcd. C, 63.39; H, 4.14; N, 13.69; Found C, 63.25; H, 4.06 ; N, 13.77%. Mass (m/z), $(M+H)^{+,}$ (512.4) (**Supplementary Materials, Fig. S19**). FT-IR spectrum, ν_{max} (cm^{-1}): 1106, ν(C-O); 1467, ν(N=N); 1607, ν(C=N); 3387, ν(O-H); 1175, ν(S-O) (**Supplementary Materials, Fig. S20**); ^1H NMR spectrum, (DMSO-d_6) δ(17-CH_3)(oxazole), 2.48 (s); δ(16-H), 8.15 (s); δ(O-H), 13.9 (s); δ(N-H), 6.15 (s); δ(CH-N), 9.21 (s); δ(4-H), 7.20 (d, J = 8.83 Hz); δ(5-H), 7.60 (d, J = 7.7 Hz); δ(7-H), 7.50 (s); δ(10,12-H), 7.90 (m); δ(9,13-H), 8.20 (m); δ(Hs of naphthyl) 7.75-7.96 (m) (**Supplementary Materials, Fig. S-21**).

2.3. X-Ray crystal structure analysis of SMX-N=N-C_6H_3(*p*-OH)(*m*-CH=N-C_6H_4-*p*-OCH_3), (**2c**)

The crystals of **2c** were obtained by slow evaporation of methanol solution (0.12 x 0.10 x 0.02 mm^3) for a week. Data were collected by Bruker Smart CCD Area Detector at 173(2) K with θ in the range 2.429° ≤ θ ≤ 25.35°. Fine-focus sealed tube was used as the radiation source of graphite-monochromatized Mo-Kα radiation (λ = 0.71075 Å). Empirical absorption correction in the *h k l* range: -22 ≤ *h* ≤ 22, -8 ≤ *k* ≤ 8, -22 ≤ *l* ≤ 22 was accomplished with the program SADABS [18]. Crystallographic refinement data are collected in **Table 1**. Multi-scan absorption corrections were applied [19]. The structure was solved by direct methods with SHELXL-97 [20] and refined by full-matrix least-squares techniques on F^2 using the SHELXS-97 [21] program with anisotropic displacement parameters for all non-hydrogen atoms. The ORTEP-3 [22] was used within WinGX to prepare figures and tables for publication. Hydrogen atoms were constrained to ride on the respective carbon atoms with isotropic displacement parameters equal to 1.2 times the equivalent isotropic displacement of their parent atoms in all cases of aromatic units. Residual minimum and maximum electron densities are -0.350 and 0.440.

2.4. Antimicrobial activity

[SMX-N=N-C_6H_2-(*p*-OH)(*m*-CHO)] (**1**) and its six derivatives SMX-N=N-C_6H_3(*p*-OH)(*m*-CH=N-C_6H_5) (**2a**), SMX-N=N-C_6H_3(*p*-OH)(*m*-CH=N-C_6H_4-*p*-CH_3) (**2b**), SMX-N=N-C_6H_3(*p*-OH)(*m*-CH=N-C_6H_4-*p*-OCH_3) (**2c**), SMX-N=N-C_6H_3(*p*-OH)(*m*-CH=N-C_6H_4-*p*-Cl) (**2d**), SMX-N=N-C_6H_3(*p*-OH)(*m*-CH=N-C_6H_4-*p*-NO_2) (**2e**), SMX-N=N-C_6H_3(*p*-OH)(*m*-CH=N-(α)-$C_{10}H_7$) (**2f**) were tested against gram positive, *B. subtillis* (ATCC 6633) and gram negative, *E. coli* (ATCC 8739) bacteria. The compounds were dissolved in HPLC grade DMSO; final % of DMSO during assay was varied from 0.5-0.8% although the main stocks of the drugs were

Table 1: Crystal data and structure refinement of SMX-N=N-C_6H_3(*p*-OH)(*m*-CH=N-C_6H_4-*p*-OCH_3) (**2c**)

	2c
Empirical formula	$C_{24}H_{21}N_5O_5S$
Formula weight	491.52
Temperature (K)	173
Crystal system	Monoclinic
Space group	P2/c
a(Å)	18.285(5)
b(Å)	6.8187(16)
c(Å)	18.507(5)
β (°)	103.745(4)
V(Å)^3	2241.4(10)
Z	4
μ (MoK$_\alpha$) (mm^{-1})	0.71075
θ range	2.29 – 25.35
D_{calc} (mg m^{-3})	1.456
Refine parameters	324
Total reflections	4084
Unique reflections	21015
R_1[a] [I > 2σ (I)]	0.0497
wR_2[b]	0. 1190
GOF[c]	1.083

[a]$R = \Sigma \left| F_0 - F_c \right| / \Sigma F_0$. [b]$wR = [\Sigma w(F_0^2 - F_c^2) / \Sigma w F_0^4]^{1/2}$ are general but *w* are different, w = 1/ $[\sigma^2 (F_o^2) + (0.0508P)^2 + 1.7997P]$ where $P=(F_o^2+2F_c^2)/3$

prepared using spectroscopic grade DMSO and stored at -20°C. All the bacterial strains were inoculated in a freshly prepared autoclaved LB broth from a 24 hours old LA slant and kept in shaker for overnight. From the overnight culture it was diluted to a final bacterial count of 1x 10^4 cells /ml with sterile LB. The diluted culture was distributed in a number of tubes and incubated in absence as well as in presence of various concentrations of test compounds. All the tubes were incubated for 16-18 hours at 37°C in shaking condition. The OD_{600} had been measured in a UV visible spectrophotometer (Shimadzu). The OD value observed in absence of test ligand had been considered as control with 100 % growth for both the bacterial species. Compared to control the relative degree of bacterial growth inhibition had been calculated for each concentration incubated under similar experimental condition from a measurement of OD at 600 nm. The minimum inhibitory concentrations (IC_{50}) *i.e.* the concentration of test compound required to inhibit the growth of bacteria by 50 % had been calculated from the % reduction of bacterial growth in comparison to control.

2.5. MTT assay

Vero cells (African green monkey kidney cells; ATCC, Manassas, VA, USA) were cultured in Dulbecco's modified Eagle's medium (DMEM) with 5–10% fetal bovine serum (FBS; Invitrogen, USA), 100 U ml^{-1} penicillin and 100 mg ml^{-1} streptomycin, at 37 ^{0}C in 5% CO_2. The viral strains used were HSV-1F (ATCC 734), purchased from the ATCC (Manassas, VA, USA). Virus stocks were prepared from infected culture at a multiplicity of infection (MOI) of 0.5 to 1 h at 37°C. The residual viruses were then washed out with phosphate-buffered saline (PBS) and the cells were cultured for another 48–72 h. The cultured cells were lysed finally by three cycles

of freezing and thawing, centrifuged at 4°C for 20 min and the collected supernatant was tittered by plaque assay, and stored at -80°C for further studies.

The effect of compounds on African green monkey kidney cells (Vero cell) morphology was determined by MTT (3-[4,5-dimethylthiazol-2-yl]-2,5 diphenyltetrazolium bromide) assay following the manufacturer's instruction (MTT 2003, Sigma-Aldrich). Vero cells were cultured onto 96-well plates at 10 $\times 10^6$ cells per well, and different concentrations of the compounds (**1, 2**) were added to each well at a final volume of 100 µl, in triplicate using DMSO (0.1%) and acyclovir (0–50 µg ml^{-1}) as a negative and positive control, respectively. The drug-treated cells were incubated at 37°C with 5% CO_2 for 2 days, and then the MTT reagent (10 µl) was added to each well. After 4 h of incubation, the formazan was solubilized by adding MTT solubilisation solution equal to the original culture media volume, and the absorbance was read at 570 nm with a reference wavelength of 690 nm by an ELISA reader. Data were calculated as the percentage of cell viability by the formula: [(sample absorbance cell free sample blank)/mean media control absorbance)]/100%. The 50% cytotoxic concentration (CC_{50}) causing visible morphological change in 50% of Vero cells with respect to cell control was determined [23, 24].

2.6. Anti-HSV Activity

Dose response analysis of test compounds on virus infected cell was done to observe the viral activity. Vero cells seeded in 96 well plates were infected with HSV-1F at 1 MOI and exposed to the various concentrations of **1** and **2** and acyclovir (standard drug). The dose-dependent antiviral activity was evaluated by MTT assay to determine the inhibition of infection, as described previously [25, 26]. Values were obtained from three independent experiments with each sample performed in triplicate.

2.7. Theoretical Calculation: DFT and Docking studies

The geometry optimization of **1** and **2a-f** were carried out using Density Functional theory (DFT) at the B3LYP level [27]. All calculations were carried out using the Gaussian 09 program package [28] with the aid of the GaussView visualization program [29]. For C, H, N, O the 6-31G (d) basis set were assigned. The vibrational frequency calculations were performed to ensure that the optimized geometries represent the local minima and there are only positive eigen values. Vertical electronic excitations based on B3LYP optimized geometries were computed using the time-dependent density functional theory (TD-DFT) formalism in methanol using conductor-like polarizable continuum model (CPCM) [30 – 32] Gauss Sum was used to calculate the fractional contributions of various groups to each molecular orbital [33].

The crystal structure of DHPS (Dihydroptorat Synthetase of *Versinia pestis*, PDB ID 3TZF) was downloaded from RCSB protein data bank (http://www.pdb.org) and used for docking. The enzyme was co-crystallized with sulfamethoxazole, 6-hydroxymethylpterin-diphosphate and magnesium ion. The *in silico* docking studies was carried out by using CDOCKER of Receptor-Ligand interactions protocol section of Discovery Studio client 3.5 [34]. Interaction energies between Ligands and Receptor were recorded. Lipinski's rule [35] and Veber rule [36] were verified and the drugs were passed though ADMET for toxicity computation.

The crystal structure of **2c** and optimized structures of other compounds (**1**, **2a-f**) have been used for docking. Ligand preparation was done using Prepare Ligand module in Receptor-Ligand interactions tool of Discovery studio 3.5 and prepared ligand was used for docking. Protein preparation was done under Prepare Protein module of Receptor-Ligand interactions tool of Discovery Studio 3.5 and that was used for docking. The active site was selected based on the ligand binding domain of sulfamethoxazole then the pre-existing ligand was removed and

prepared ligand, was placed. Most favorable docked pose was selected according to the minimum free energy of protein-ligand complex and analyzed to investigate the interaction. Absorption, distribution, metabolism, excretion and toxicity (ADMET) prediction were done in ADMET descriptor module of Small molecules protocol of Discovery studio client 3.5. Druglikeness of the compounds used in this work was checked following Lipinski's rule of five [35]. Using ADMET module of small molecule protocol of Discovery studio 3.5 software ADMET properties and toxicity of the compounds were checked.

3. Results and discussion

3.1. Synthesis and spectroscopic characterisation

4-(3-Formyl-4-hydroxy-phenylazo)-N-(5-methyl-isoxazol-3-yl)-benzene sulfonamide [SMX-N=N-C_6H_3-(*p*-OH)(*m*-CHO)] (**1**) reacts with aromatic amines, *p*-R-C_6H_4-NH_2, to synthesize SMX-N=N-C_6H_3(*p*-OH)(*m*-CH=N-C_6H_4-*p*-R)) (R = H (**2a**), -CH_3 (**2b**), -OCH_3 (**2c**), -Cl (**2d**), -NO_2 (**2e**), -α-naphthyl (**2f**)). Disappearance of ν(CHO) at 1659 cm^{-1} of **1** in the FT-IR spectra of the products, **2**, and the emergence of strong stretch at 1610 – 1625 cm^{-1} refer to ν(HC=N) are in support of the condensation reaction. Other significant stretches such as ν(N=N), 1470-1480; ν(C-O), 1090–1110; ν(SO_2), 1170-1180 cm^{-1} support the synthesis of the compounds **2** (**Supplementary material, Fig. S2, S5, S8, S11, S14, S17, S20**). The mass spectra identify the molecular ion peak which also support the calculated m/z and have established the isolation of **2.** All the compounds show absorption bands at 350-370 nm and 270-290 nm due to n-π^* and π-π^* transitions, respectively (**Fig. 1**). The ^{1}H NMR spectra are convoluted due to large number of proton signals from aromatic rings (atom numbering is given in the structures, **Scheme 1**); however significant singlet signals are oxazolyl-CH_3 (2.45-2.50 ppm), δ(OH) (11.40 – 11.50 ppm), δ(NH) (6.10 – 6.20 ppm); δ(CH=N), 9.10 – 9.20 ppm. Oxazolyl-H (16-H, singlet)

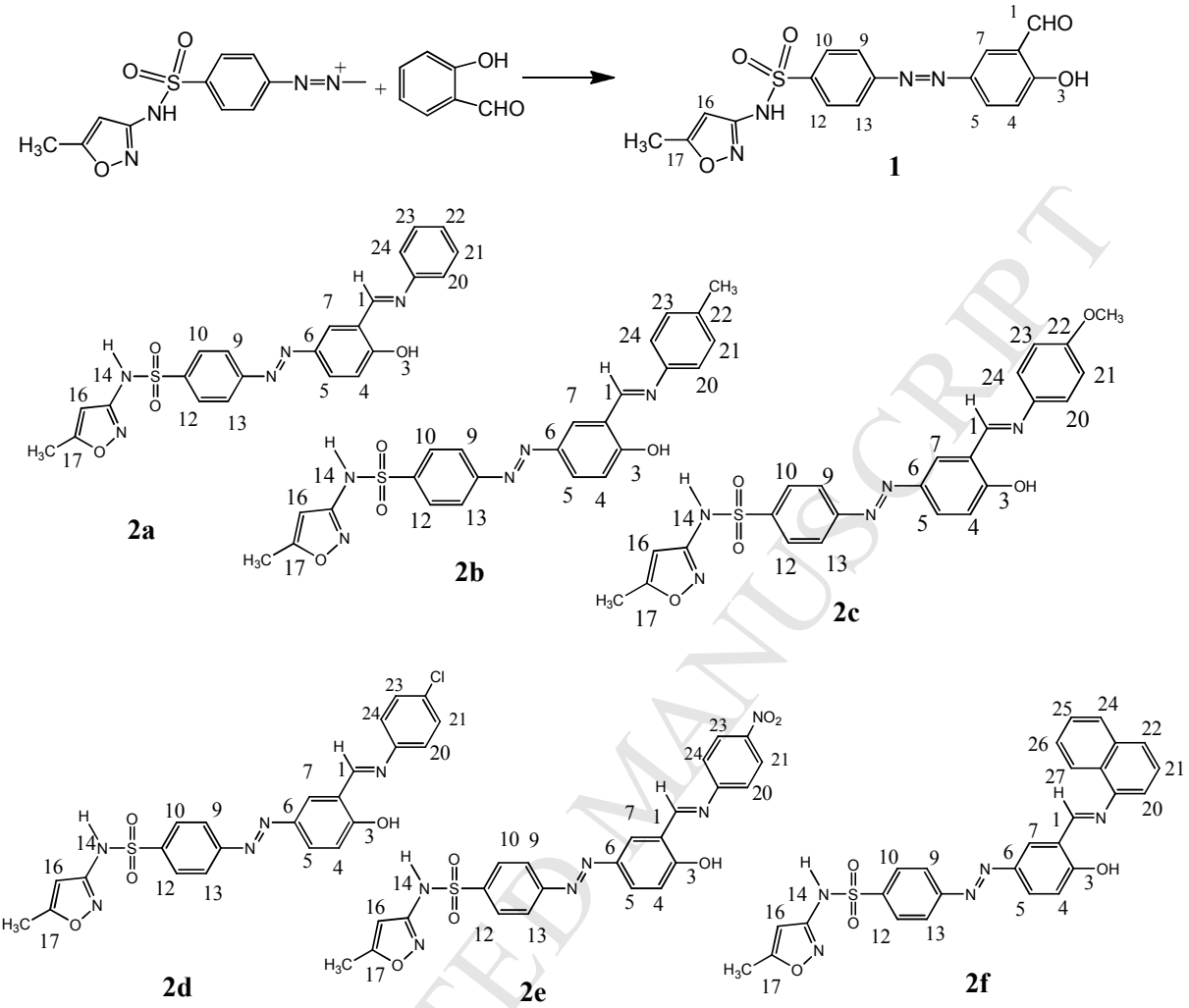

Scheme 1. Synthesis of SMX-azo-imine derivatives; SMX-N=N-C_6H_3(*p*-OH)(*m*-CHO) (**1**), SMX-N=N-C_6H_3(*p*-OH)(*m*-CH=N-C_6H_5) (**2a**), SMX-N=N-C_6H_3(*p*-OH)(*m*-CH=N-C_6H_4-*p*-CH_3) (**2b**), SMX-N=N-C_6H_3(*p*-OH)(*m*-CH=N-C_6H_4-*p*-OCH_3) (**2c**), SMX-N=N-C_6H_3(*p*-OH)(*m*-CH=N-C_6H_4-*p*-Cl) (**2d**), SMX-N=N-C_6H_3(*p*-OH)(*m*-CH=N-C_6H_4-*p*-NO_2) (**2e**), SMX-N=N-C_6H_3(*p*-OH)(*m*-CH=N-(α)-$C_{10}H_7$) (**2f**).

appears at 8.29-8.31 ppm and sulfonamide-phenyl-Hs (9,10,12,13-H) become visible as two doublets at 7.35 – 7.45 ppm. Azophenolato-H such as 7-H is a singlet at 7.10-7.15 ppm while 4,5-H show doublet signal at 7.10 – 7.30 ppm. The terminal six member ring, arylamine has four

or five-Hs and have shown noteworthy signal movement due to substituent effect; electron donating $–CH_3$ and $-OCH_3$ influence 21,23-H to shift to upfield side while electron withdrawing groups –Cl and $–NO_2$ influence them to move to downfield side (**Supplementary material, Fig. S12, S18**). The single crystal X-ray structure of **2c** also confirms the structural proposal from other spectroscopic information.

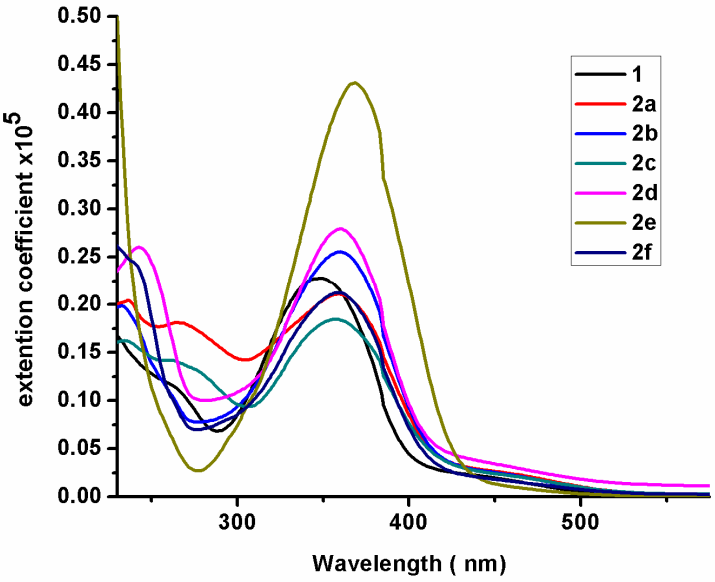

Fig. 1. Electronic spectra of the compounds, **1** and **2a-f** in methanol solution

3.2. Molecular structure of 2c

An ORTEP view of **2c** is shown in **Fig. 2**. The selected bond lengths and angles are given in **Table 2**. The structure is sub-divided into four parts for brevity; imine phenolato (A-ring), aryl-sulfonamide (B-ring) oxazolyl (C-ring), methoxy substituted phenyl (D ring). The C-ring is linked to B-ring by the sulfonamide ($-NH-SO_2-$) group and the B-ring is connected to A-ring by –N=N- group and A ring is attached to D -ring by -HC=N- group. The $-C_6H_3(OH)-$ (A-ring) and $-C_6H_4(SO_2)-$) (B-ring) are bonded to –N=CH- with dihedral 15.88(13)°; oxazolyl ring

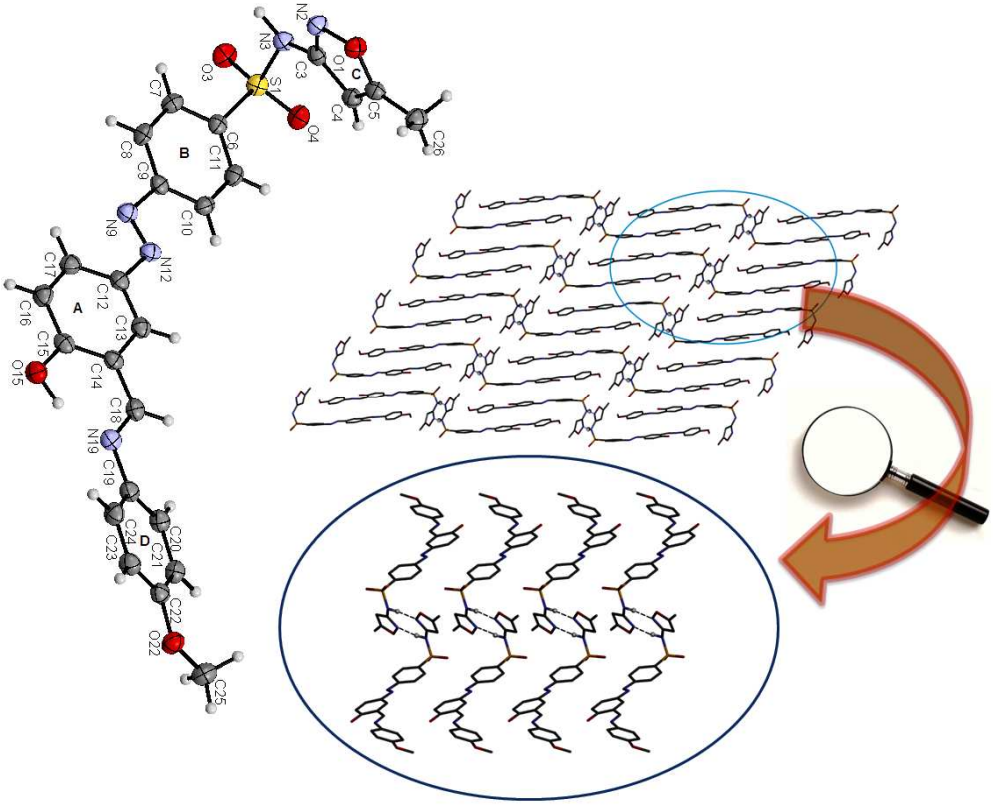

Fig. 2. ORTEP structure (30% ellipsoid) and hydrogen bonded 1D chain followed by π---π interaction to build 2D network (aromatic rings are marked : A, imine phenolato ring; B, aryl-sulfonamide ring; C, oxazolyl ring; D, methoxy substituted phenyl ring).

(C-ring) is inclined at 88.16(17)° with B-ring. The, N=N, azo length is 1.261(3) Å and the, C=N, imine length is 1.289(3) Å and these are closer to the reported data [12-15]. An intramolecular hydrogen bond -N=N-C_6H_3O–H---N-C_6H_4-*p*-OCH_3 *i.e.* (O–H---N), ∠O(15)–H(15)---N(19), 154.48(2)°; H(15)---N(19), 1.659(4) Å; O(15)---N(19), 2.580(4) Å) improves the bonding strength in the molecule. Two adjacent molecules constitute a dimer of eight-member supracycle through intermolecular hydrogen bonds N(19)-H(15), 2.580 Å. These dimers are then hydrogen bonded to consititue 1-D chain *via* N(2)-H(3), 1.926 Å. Two aryl rings, imine phenolato (A-ring)

of two adjacent molecules show cross π---π interaction, A---B, 4.02 Å (**Fig. 2**). In the expanded structure both intramolecular and intermolecular hydrogen bonds constitute 2D plane. Hydrogen bonded centres are –O-CH_3, -OH, -SO_2-NH-, azo-N, oxazolyl-N, phenyl-Hs, -CH_3 group in oxazolyl motif.

The optimized structure generated by DFT computation using Gaussian09 package for **2c** has been verified from the bond parameters with experimentally determined single crystal X-ray structure (**Fig. 2**, **Table 2**). Theoretically generated bond parameters such as N(9)–N(12) (1.248 Å), C(9)-N(9) (1.459 Å), C(6)-S(1) (1.790 Å), differ by 0.004-0.03 Å and the bond angles ∠N(9)–N(12)–C(12), 107.5°; ∠N(12)–C(12)–C(17), 119.9°; ∠O(4)–S(1)–C(6), 109.5° differ by 2-4°. This closeness in the metric parameters supports high agreement in the calculated molecular functions of the molecule.

Table 2: Selected bond lengths and bond angles of **2c**

SMX-N=N-C_6H_3(*p*-OH)(*m*-*H*C=N-C_6H_4(*p*-OCH_3)) (2c)					
Bond length (Å)			Bond Angle (°)		
	X-Ray	DFT		X-Ray	DFT
N(9)–N(12)	1.261(3)	1.248	N(9)–N(12)–C(12)	114.4(2)	107.5
C(9)-N(9)	1.425(3)	1.459	C(9)–N(9)–N(12)	112.9(2)	107.4
C(12)-N(12)	1.416(3)	1.390	N(12)–C(12)–C(17)	124.9(2)	119.9
C(18)-N(19)	1.419(3)	1.386	N(9)–C(9)–C(10)	123.7(2)	120.0
N(19)-C(18)	1.289(3)	1.260	C(18)–N(19)–C(19)	121.4(2)	115.0
C(6)-S(1)	1.763(2)	1.790	N(19)–C(18)–C(14)	121.1(2)	120.0
C(9)-C(10)	1.391(3)	1.395	O(4)–S(1)–C(6)	107.8(1)	109.5

3.3. Antimicrobial activity

The interaction of PABA with DHPS is crucial for bacterial folic acid synthesis which is being interfered by SMX and is popularly known as antimicrobial activity. During metabolic process SMX is oxidized to toxic metabolic products by Cyt P450 and the end products are responsible for hypersensitivity and toxicity. The compounds, [SMX-N=N-C_6H_3-(*p*-OH)-(*m*-CHO)] (**1**) and their six Schiff bases SMX-N=N-C_6H_3(*p*-OH)(*m*-CH=N-C_6H_5) (**2a**), SMX-N=N-C_6H_3(*p*-OH)(*m*-CH=N-C_6H_4-*p*-CH_3) (**2b**), SMX-N=N-C_6H_3(*p*-OH)(*m*-CH=N-C_6H_4-*p*-OCH_3) (**2c**), SMX-N=N-C_6H_3(*p*-OH)(*m*-CH=N-C_6H_4-*p*-Cl) (**2d**), SMX-N=N-C_6H_3(*p*-OH)(*m*-CH=N-C_6H_4-*p*-NO_2) (**2e**), SMX-N=N-C_6H_3(*p*-OH)(*m*-CH=N-(α)-$C_{10}H_7$) (**2f**) have been tested against gram positive, *B. subtillis* (ATCC 6633) and gram negative, *E. coli* (ATCC 8739) bacteria. The OD value (600 nm) observed in absence of test ligand and had been considered as control with 100 % growth for both the bacterial species. The minimum inhibitory concentrations (IC_{50}) *i.e.* the concentration of test compound required to inhibit the growth of bacteria by 50 % for **1** and **2** have been tested against *B. subtillis* (ATCC 6633) and *E. coli* (ATCC 8739) (**Table 3**). Data reveal that Schiff bases **2** are less potent than that of the precursor aldehyde, **1;** the reason is unknown. However, one may apprehend that –CHO is more polar and less space demanding than –CH=N-Ar and may be easily permeable in the cell membrane [37]. The profile of inhibition has been presented in **Fig. 3**. From the result it is evident that the drug molecules produce a concentration dependant decrease in the growth of gram positive, *B. Subtillis* but not in gram negative, *E.coli.*

3.4. Inhibition of HSV-1F infection

The cytotoxicity assay of the compounds indicated that 50% drug efficiency (CC_{50}, µg/ml) of the drugs are 129.98 (**1**), 74.36 (**2a**), 93.01 (**2b**), 191.97 (**2c**), 99.1 (**2d**), 93.18 (**2e**) and 61.98 (**2f**).

The antiviral effects of each drug is examined against HSV-1-infected Vero cells (MOI 1) by MTT assay, using acyclovir as positive and DMSO (0.1%) as negative control. The results reveal that the drug **1** could inhibit virus in a dose dependent manner, but the derivatives **2** have shown less anti-HSV potential as well as EC_{50} activity (the 50% effective concentration) for HSV-1. The selectivity index (SI), a measure of the preferential antiviral activity of a drug in relation to its cytotoxicity (CC_{50}/EC_{50}), of the compounds are 5.06 (**1**), 1.18 (**2a**), 1.42 (**2b**), 3.50 (**2c**), 1.45 (**2d**), 1.58 (**2e**), 1.29 (**2f**) and 52.48 (acyclovir) against HSV-1. Thus, the precursor **1** is selected as best antiviral compound amongst drugs tested in this work. Acyclovir achieved >99% inhibition at 5 mg ml^{-1} for HSV-1. The result (**Fig. 4**) has revealed that the drugs **1** and **2a-f** have inhibited HSV-1 in a dose-dependent manner. The derivatives, **2a-f** are inactive as their SI values are less than 4 while the precursor **1** is considered as active against HSV infection because of Selectivity Index (SI) (CC_{50}/ EC_{50}) is 5.06.

Table 3: Half-maximal Inhibitory Concentrations (IC_{50}) of **1** and **2** against *B. Subtilis* and *E. coli*

	B. Subtilis (µg/ml)	*E. coli* (µg/ml)
SMX	101.0	95.0
1	39.3	159.0
2a	60.1	151.4
2b	64.0	155.3
2c	85.6	140.0
2d	55.2	156.0
2e	88.4	153.5
2f	65.2	157.0

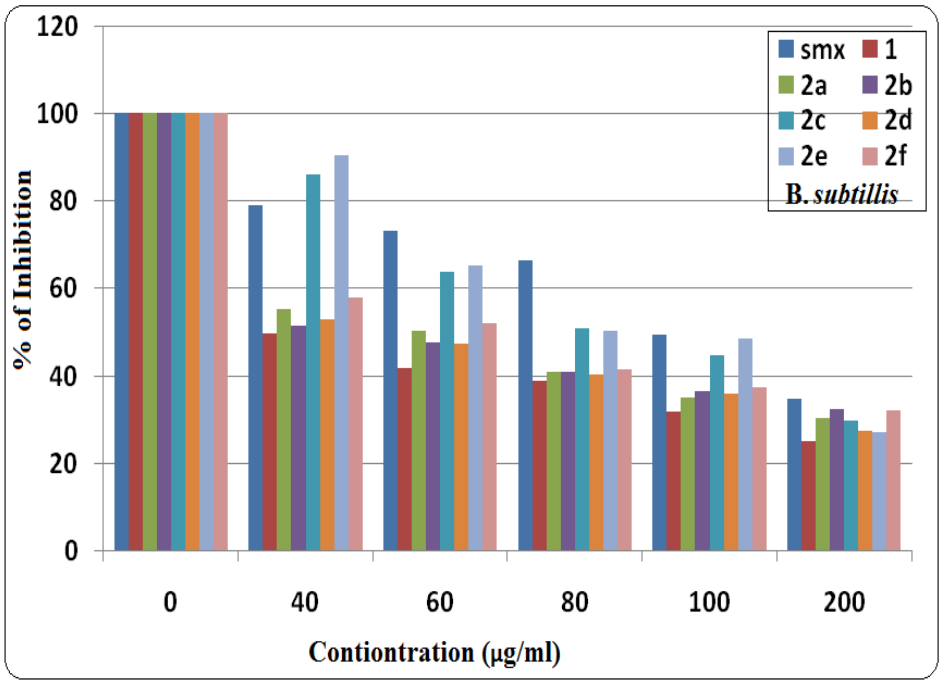

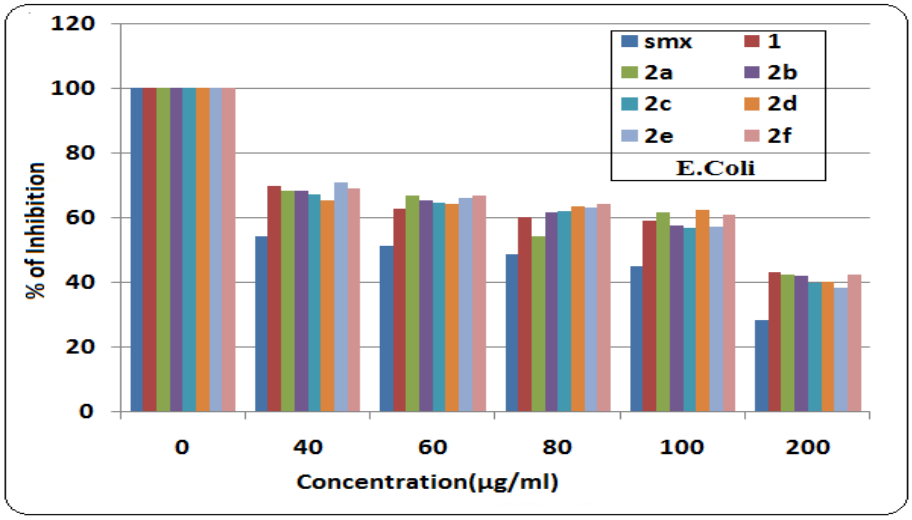

Fig. 3. Inhibition profile of SMX, [SMX-N=N-C_6H_3-(*p*-OH)-(*m*-CHO)] (**1**) and their six derivative [SMX-N=N-C_6H_2-(*p*-OH)-(*m*-HC=N-Ar)] (Ar : **– C_6H_5 (2a)**, **– C_6H_4-(*p*-CH_3) (2b)**, **– C_6H_4-(*p*-OCH_3) (2c)**, **– C_6H_4-(*p*-Cl) (2d)**, **– C_6H_4-(*p*-NO_2) (2e)**, **-$C_{10}H_7$ (2f)** for *B. subtillis* and *E. coli*

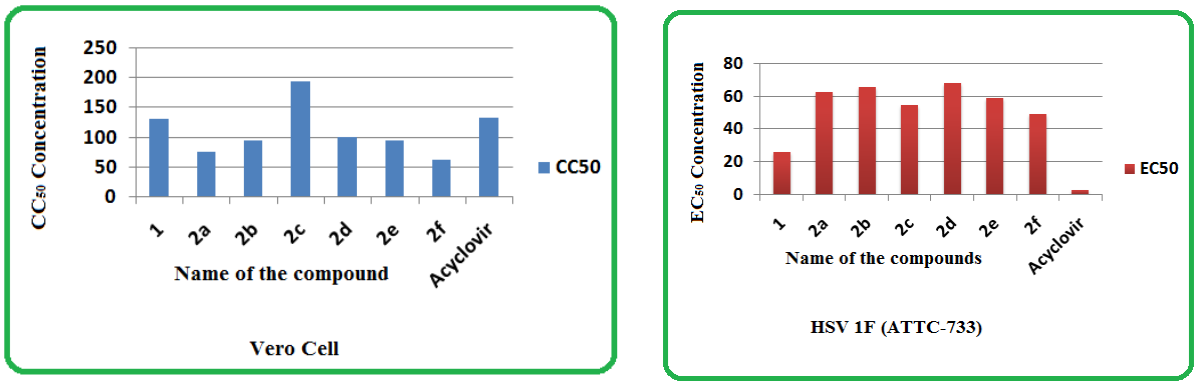

Fig. 4. Half-effective concentration (EC_{50}) and selectivity index (SI) of **1** and **2** against HSV-1F infection (The 50% cytotoxicity concentration for Vero cell in µg ml^{-1}, concentration of compound (µg ml^{-1}) producing 50% inhibition of virus induced CPE of three separate experiments. Selectivity index (SI), CC_{50}/EC_{50}).

3.5. Theoretical Interpretation by DFT and Docking studies

The DFT optimized structures or the structure obtained from the single crystal X-ray analysis are useful to study protein ligand interaction. The best pose interaction has been evaluated by docking score, binding energy and Log P data. To follow Lipinski's rule of five, (35,36) it is essential to know drug-relevant properties of the ligands. Finally the druglikeness of the target molecules has been tested by ADMET to know the molecular properties *i.e.* absorption, distribution, metabolism, excretion and toxicity. The calculated data show the good solubility level, moderate absorption stage, seven or eight H-bond acceptors, two H-bond donors and follow Lipinski's filter and Log Ps vary from 3.431 to 6.161 (**Table 5**). This implies that present series of azo-sulfonamids / azo-imino-sulfonamids interact more strongly than that of SMX to DHPS protein (**Table 4**). The hydrophilic and hydrophobic parts of the derivatives bind through hydrogen bonding and different electrostatic interactions [37, 38].

Table 4: Iinteractions energy in most stable protein-ligand complex for **1** and **2**

Compounds	CDOCKER interaction Energy (a.u.)	Binding energy (Kcal/mol)	Ligand energy (Kcal/mol)	Protein energy (Kcal/mol)	Energy of protein ligand complex (Kcal/mol)
3TZF@**1**	-42.58	-87.47	22.67	-22,831	-22,896
3TZF@**2a**	-49.61	-90.31	11.78	-22,831	-22,835
3TZF@**2b**	-51.11	-98.91	12.10	-22,831	-22,918
3TZF@**2c**	-48.89	-115.89	10.64	-22,831	-22,936
3TZF@**2d**	-42.96	-108.44	19.23	-22,831	-22,920
3TZF@**2e**	-43.47	-84.23	20.61	-22,831	-22,748
3TZF@**2f**	-49.90	-104.18	35.48	-22,831	-22,900

Data in **Table 4** reveal that the C-DOCKER interaction energy of the drugs with 3TZF follow the ordering **2b**>**2f**>**2a**>**2c**>**2e**>**2d**>**1**; thus the ligand **2b** shows fast communication with the protein. The steps to the best interaction of the drug-to-protein are the communication to surface interaction which follows the binding to penetration into the cavity or pocket and finally the chemical and physiological transformation through metabolic process [39]. Hence C-DOCKER interaction energy trend does not reflect its binding strength; it is the binding energy which will reflect the strength of binding. The drug **2c** binds to the protein (**Table 4**), 3TZF@**2c** and shows highest stability (-115.89 Kcal/mol). The interaction proceeds mainly through electrostatic path with 3TZF. The drug **1** interacts with 3TZF (3TZF@**1**) and the amino acid residues involve in the interactions are Lys221, Ser 222, Arg255, Arg255. In case of 3TZF@**2** the amino acid residues Ser222, Lys 221, Leu193 for **2a**, Gly139, Thr62 for **2b**, Gly189 and Arg255 (NH to O of OCH_3) for **2c**, Arg255 for **2d**, Thr62 and arg255 for **2e**, Arg135 and Gly189 for **2f** are involved in the binding cavity of the protein. Interaction analysis suggests that ligand **1**

binds with DHPS of *E. coli* through oxygen atom of -SO_2, oxazolyl moiety, azo-N and form recognizable H-bonds (**Fig.5**). Lys221 NH atom interacts with -C=O of salicyldehyde moiety: H--C 1.88 Å and ∠N-H---O, 150°; Ser222-O atom interacts with NH (sulfonamide moiety): O—H, 2.87 Å and ∠O--H-N, 91°; Arg255 NH---O (salicylaldehyde): N---O, 2.20 Å; ∠N–H---O, 114°; Arg255 NH---O(salicylaldehyde) : N---O, 2.99 Å; ∠N–H---O, 110^o for **1** (**Fig. 5**) and Leu194 NH---O(SO_2) : H---O, 2.10 Å; ∠N–H---O, 145°; Ser222 CH interacts with azo-N, H----N, 2.69 Å; ∠C–H---N 135^o and Lys221 CH atom interacts with N(imine moiety), H---N, 2.69; ∠C–H---N, 157^o. Pro 64 oxazole nucleus involves π---π interaction with salicylaldehyde ring (4.36°) for **2a** (**Fig. 6**); Ser62 OH interacts with salicylaldehyde-O moiety : O---H, 2.02°; ∠H---HO 142^o of **2b** (**Fig. 7**); Gly189 O atom interacts with OH of salicylaldehyde moiety : O---O, 3.02 Å; ∠O---O-H, 117°, Arg255 NH atom interacts with O of OCH_3 moiety: H---O, 2.03 Å and ∠N-H---O, 148°) for **2c** (**Fig. 8**); Arg135 NH atom interacts with O of oxazolyl moiety: H---O, 2.83 Å and ∠N-H---O, 121°) for **2d** (**Fig. 9**); Thr62 HN atom to O of SO_2 moiety of SMX H---O, 2.81 Å; ∠N–H---O, 155°; Thr62 OH atom to HN of SO_2 moiety of SMX : H---N, 2.72 Å and ∠O---H-N, 154°; Arg255 NH atom to O of SO_2 moiety of SMX : H---O 2.81 Å, ∠N-H---O, 142° for **2e** (**Fig. 10**); Arg135 NH atom interacts with O of SO_2NH moiety: H---O, 1.98 Å; ∠N-H---O, 134°, Gly189 O atom interacts with salicylaldehyde-OH moiety: O---O, 2.06 Å; ∠O---O-H, 152° for **2f** (**Fig. 11);** Aromatic ring of naphthaldehyde of **2f** is involved in π---π interaction with ThrNH (3.17 Å) (**Table 6**).

Table 5: ADMET prediction of the compounds following Lipinski's filter

Compd	Mol. Weight	ADMET Solubility (aqueous)	ADMET solubility level	ADMET absorption level	ADMET _Log P	Molecular fractional polar surface area	No of H-bond acceptor	No. of H- bond donor	Lipniski's filter	Drug likeness inference	Ames Prediction
1	386.38	-4.699	2	2	3.343	0.393	7	2	Yes	Yes, low	Non-mutagen
2a	462.20	-6.034	2	2	3.883	0.345	7	2	yes	Yes, low	Non-mutagen
2b	475.52	-6.406	2	2	5.666	0.298	8	2	yes	Yes, Low	Non-mutagen
2c	491.52	-5.931	2	2	5.163	0.308	8	2	No	Yes, low	Non-mutagen
2d	495.94	-6.731	1	2	5.844	0.298	7	2	No	Yes, low	Non-mutagen
2e	507.50	-5.046	1	2	6.161	0.299	7	2	no	Yes, low	Non-mutagen
2f	511.55	-6.97	1	2	6.088	0.285	7	2	No	Extremely low	Non-mutagen

Table 6: Details of interactions in most stable protein-ligand complex for 1 and 2a to f.

Compounds	Hydrogen bonds					Pi bond	
	NO. of H-bond	End 1	End2	Bond distance	Angle DHA		
3TZF@**1**	4	Lys221(NH)	Carbonyl O of salicylaldehyde.	1.88	150		
		Ser222(O)	HN of sulfonamide moiety	2.87	91		
		Arg255(HN)	O of salicylaldehyde	2.20	114		
		Arg255(HN)	O of salicylaldehyde	2.99	110		
3TZF@**2a**	1	Ser222(NH)	N of azo	2.69	135	4.36	Pro64 nucleus of oxazole ring to salicylaldehyde ring
		Lys221(CH)	N of imine	2.69	157		
		Leu194(NH)	O of SO_2	2.10	145		
		Asn193(CH)	O of SO_2	2.59	113		
3TZF@**2b**	2	Gly139(C=O)	N of Azo	3.39	147	5.11	Pro64 nucleus of oxazole ring to salicylaldehyde ring
		Thr62(HO)	HO of Salicylaldehyde	2.02	177	4.93	Phe28 nucleus of benzene ring to salicylaldehyde nucleus

3TZF@**2c**	3	Gly189(O)	OH of salicylaldehyde moiety	3.02	117		
		Arg255(NH)	O of OCH3	2.03	148		
3TZF@**2d**	1	Arg255(NH)	O of oxazole moiety	2.83	121	3.80	ThrO...nucleus of oxazole ring
3TZF@**2e**	4	Thr62(HN)	O of SO_2 of SMX	2.81	155	5.28	Phe190 nucleus of benzene to oxazole ring of SMX
		Thr62(OH)	HN of SO_2	2.72	154		
		Arg255(NH)	O of SO_2	1.74	142		
				2.14	129		
3TZF@**2f**	2	ARG135(NH)	O of SO2NH	1.98	134		
		GLy189(O)	HO of salicylaldehyde moiety	2.06	152	3.17	ThrNH...nucleas of naphthaldehyde moeity

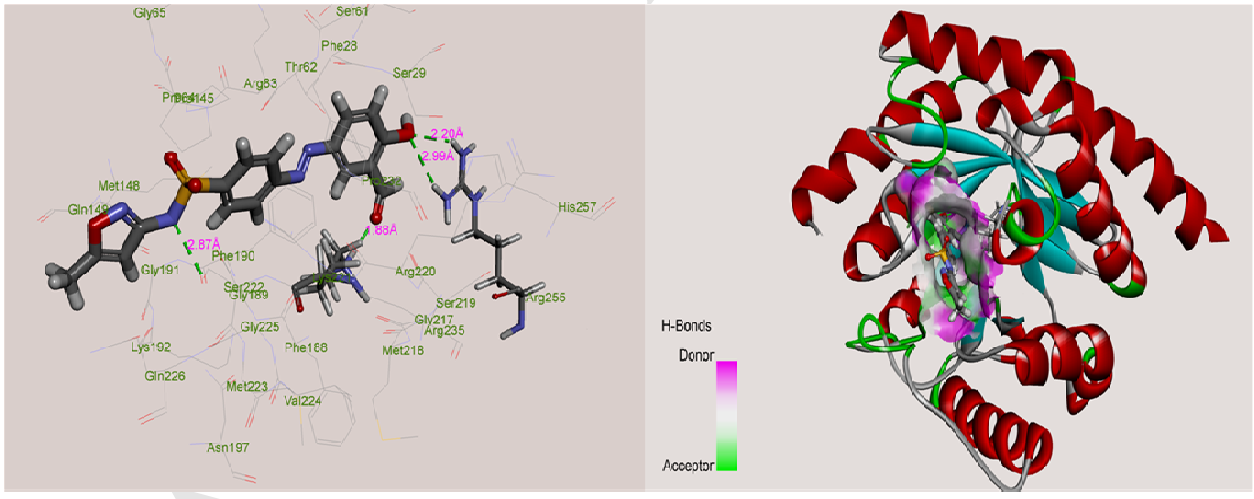

(**a**) (**b**)

Fig. 5. Best fit binding of **1** in the DHPS (PDB id 3TZF) cavity; (a) 2D interaction and (b) 3D interaction

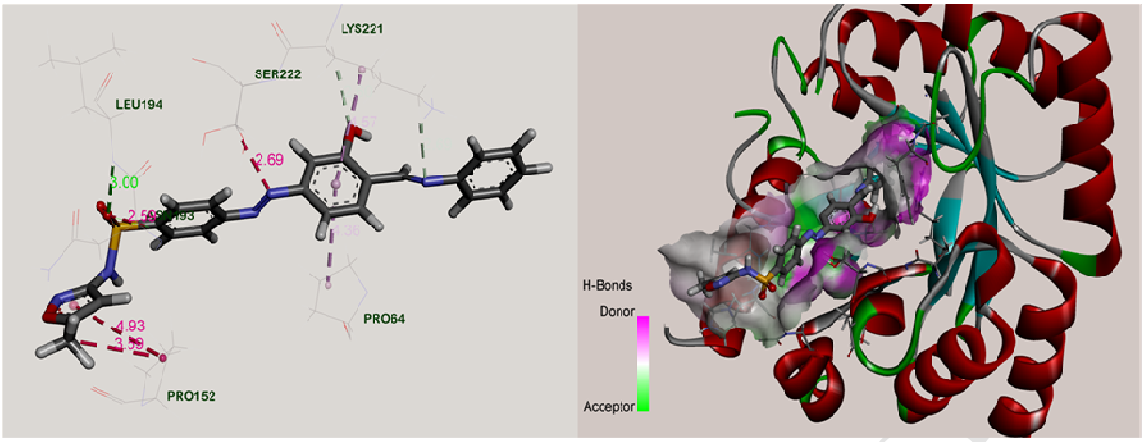

(**a**) (**b**)

Fig. 6. Best fit binding of **2a** in the DHPS (PDB id 3TZF) cavity; (a) 2D interaction and (b) 3D interaction

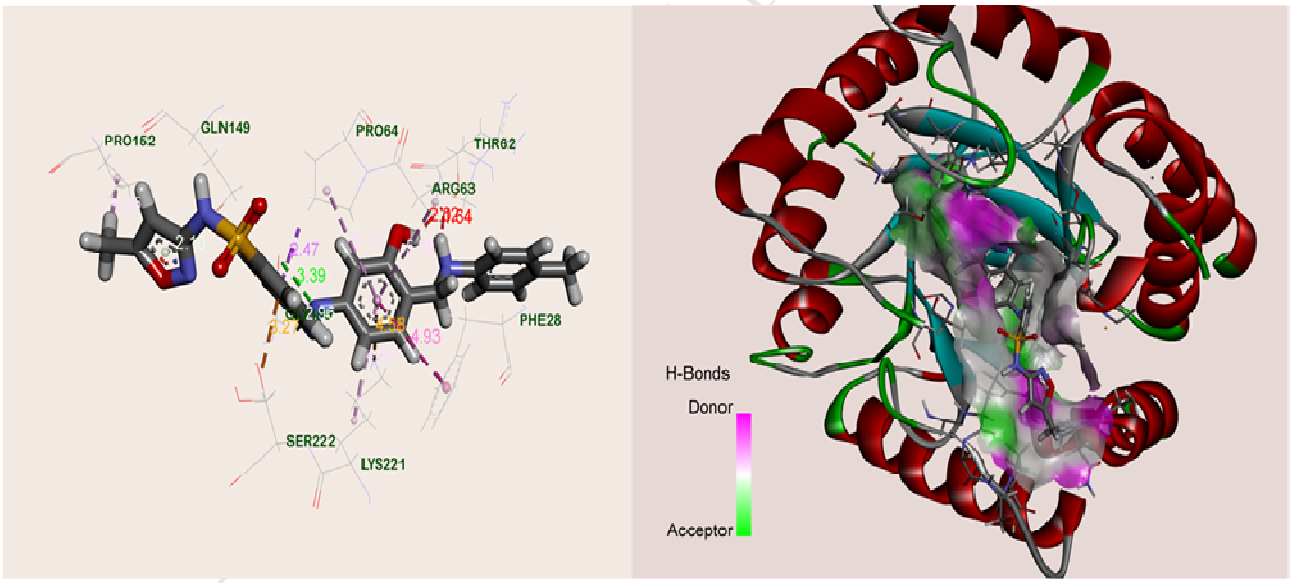

(**a**) (**b**)

Fig. 7. Best fit binding of **2b** in the DHPS (PDB id 3TZF) cavity; (a) 2D interaction and (b) 3D interaction

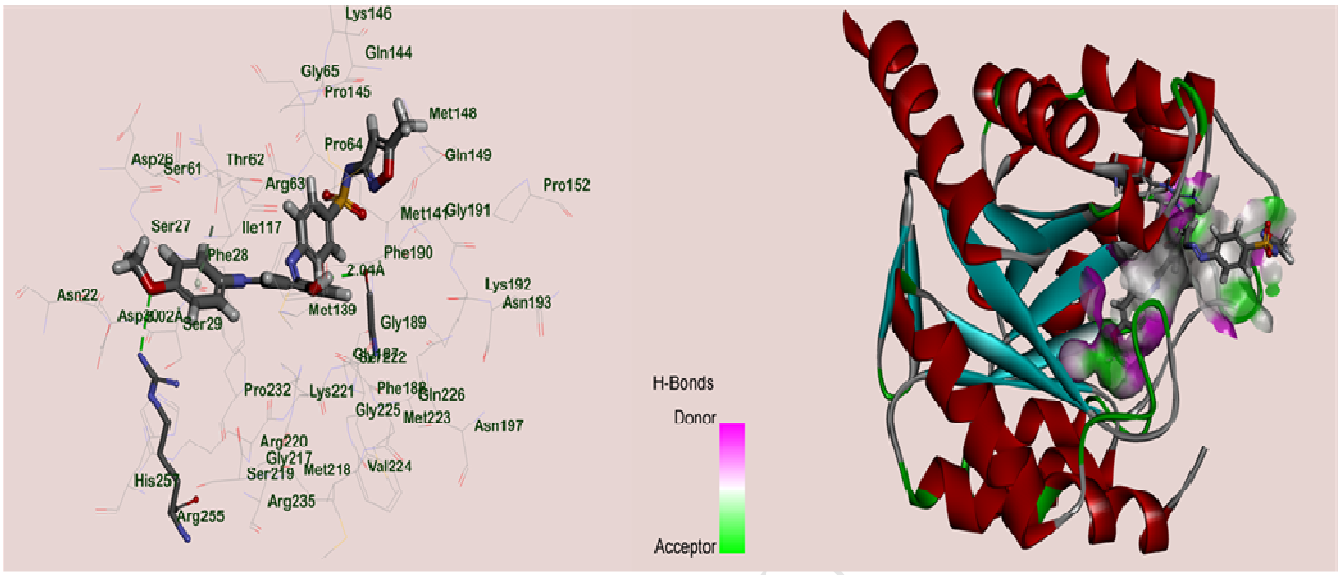

(**a**) (**b**)

Fig. 8. Best fit binding of **2c** in the DHPS (PDB id 3TZF) cavity; (a) 2D interaction and (b) 3D interaction

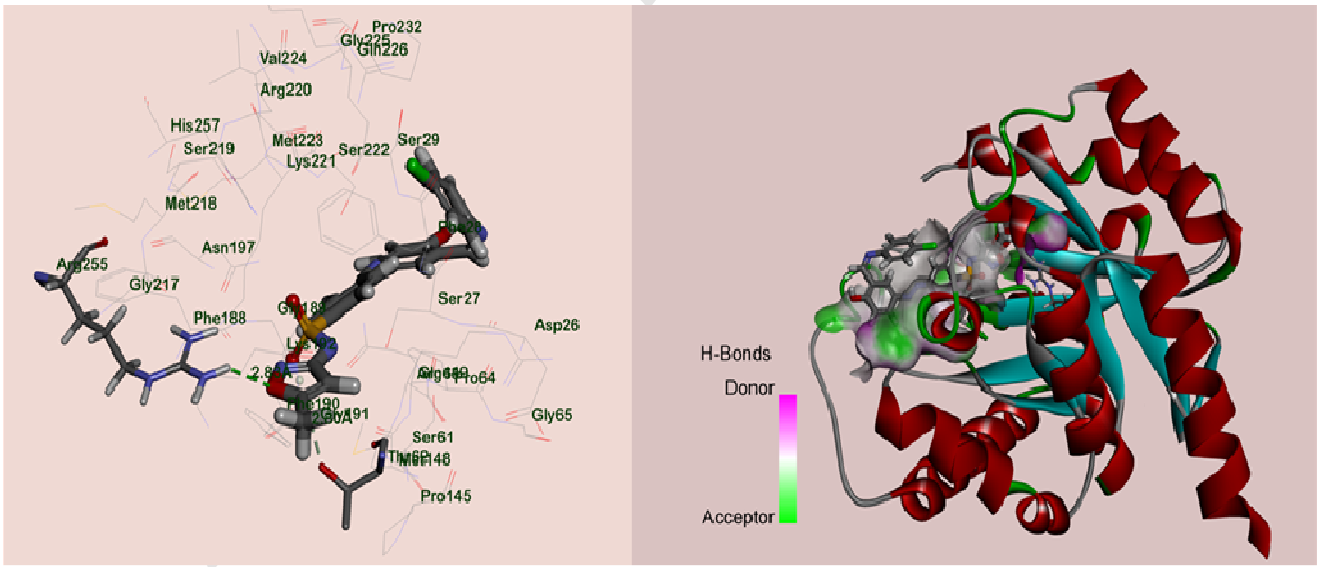

(**a**) (**b**)

Fig. 9. Best fit binding of **2d** in the DHPS (PDB id 3TZF) cavity; (a) 2D interaction and (b) 3D interaction

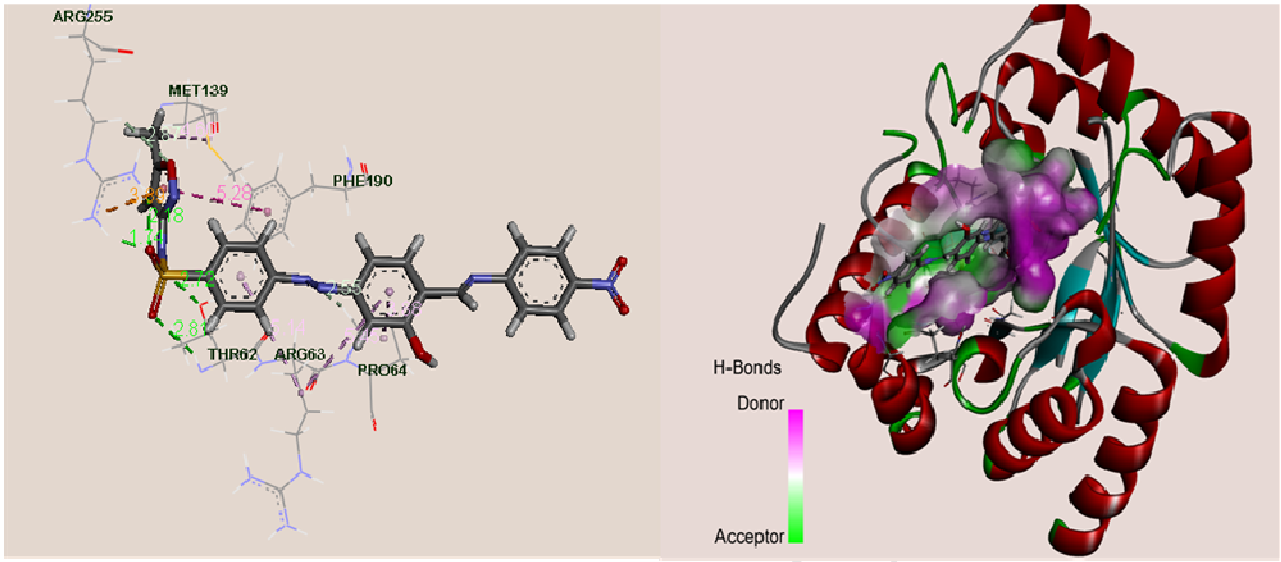

(**a**) (**b**)

Fig. 10. Best fit binding of **2e** in the DHPS (PDB id 3TZF) cavity; (a) 2D interaction and (b) 3D interaction

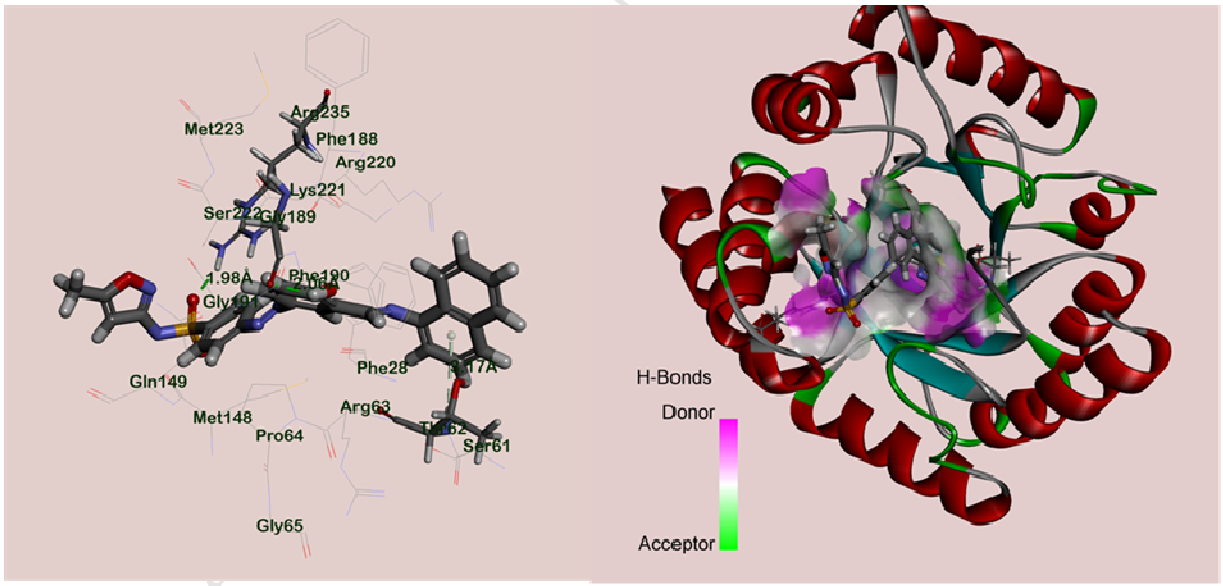

(**a**) (**b**)

Fig. 11. Best fit binding of **2f** in the DHPS (PDB id 3TZF) cavity; (a) 2D interaction and (b) 3D interaction

3.6. Theoretical interpretation of electronic spectra

The DFT computation technique is used to optimize the structure of the ligands. The bond distances and angles have been verified by the comparing between the DFT optimized and X-ray determined structures (**Table 2**). To simplify analysis of DFT computation result the structure of the ligand has been divided into azo, benzene sulfonamide (BSN), methyloxazolyl (MOX) and salicylaldehyde and aniline, *p*-toluidine, *p*-methoxyaniline, *p*-chloroaniline, *p*-nitroaniline, α-naphthylamine (**Supplementary Material, Figs. S22 – S28**). Theoretically generated structures of the ligands are used to calculate data and energy of the functions. The electronic properties of these molecules have also been verified by DFT data (**Supplementary Materials, Figs. Tables S1-S14**). The HOMO of **1** is constituted by salicylaldehyde (84%) , azo (6%), benzsulfonamide (9%) and oxazole (1%), where as **2a** is constituted by aniline (54%), azo (3%), benzsulfonamide (3%) , salicylaldehyde (60 %); **2b** is comprising toluidine (52%), azo (6%), benzsulfonamide (10%), salicylaldehyde (31%); **2c** is made up of *p*-methoxyaniline (65%), azo (1%), benzsulfonamide (1%), salicylaldehyde (33%); **2d** is composed of *p*-chloroaniline (55%), azo (3%), benzsulfonamide (6%), salicylaldehyde (36%); **2e** is formed by *p*-nitroaniline (22%), azo (8%), benzsulfonamide (1%), salicylaldehyde (66%); **2f** invol by α-naphthylamine (89%), azo (1%), and salicylaldehyde (10%).

The electronic transitions have been explained by the population of occupied MOs and unoccupied MOs. The intensity of these transitions has been assessed from oscillator strength (*f*). The ligands show transitions between different molecular fragments, *viz*., HOMO → LUMO, 458.14 nm (f, 0.915); HOMO-5 →LUMO, 319.3 nm (f, 0.2224) are considered as admixture of salicylaldehyde to

benzsulfonamide, azo charge transitions, whereas most of the accepted transitions (**Supplementary Materials, Tables S1-S14**) are intra-ligand charge transfer transitions.

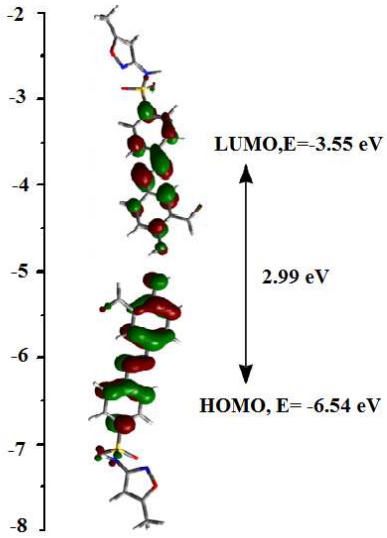

1

(**a**)

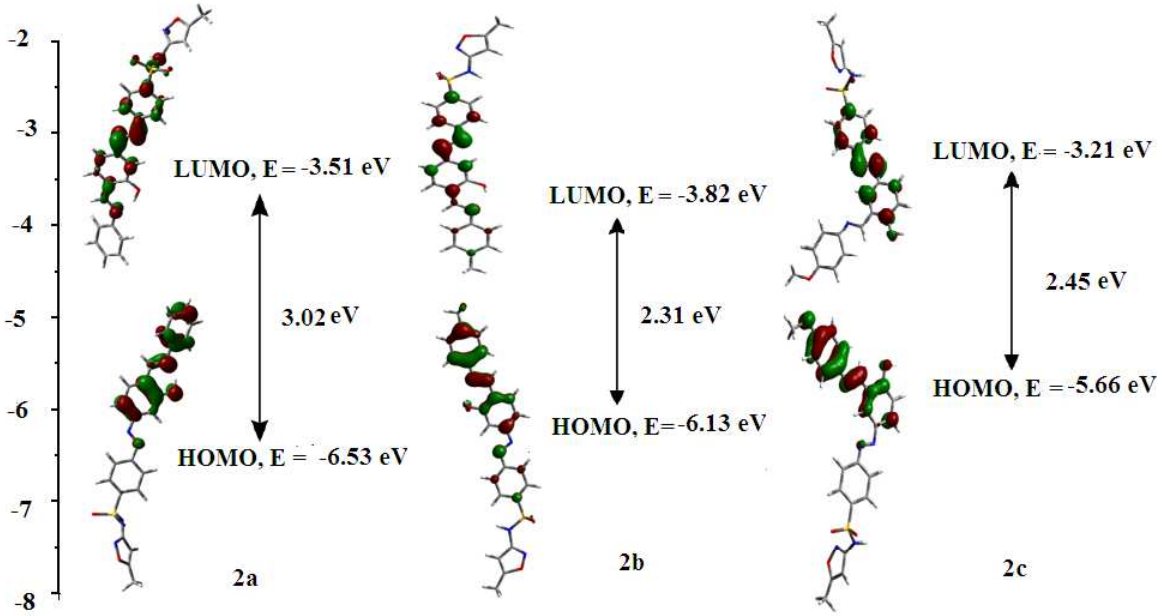

(**b**)

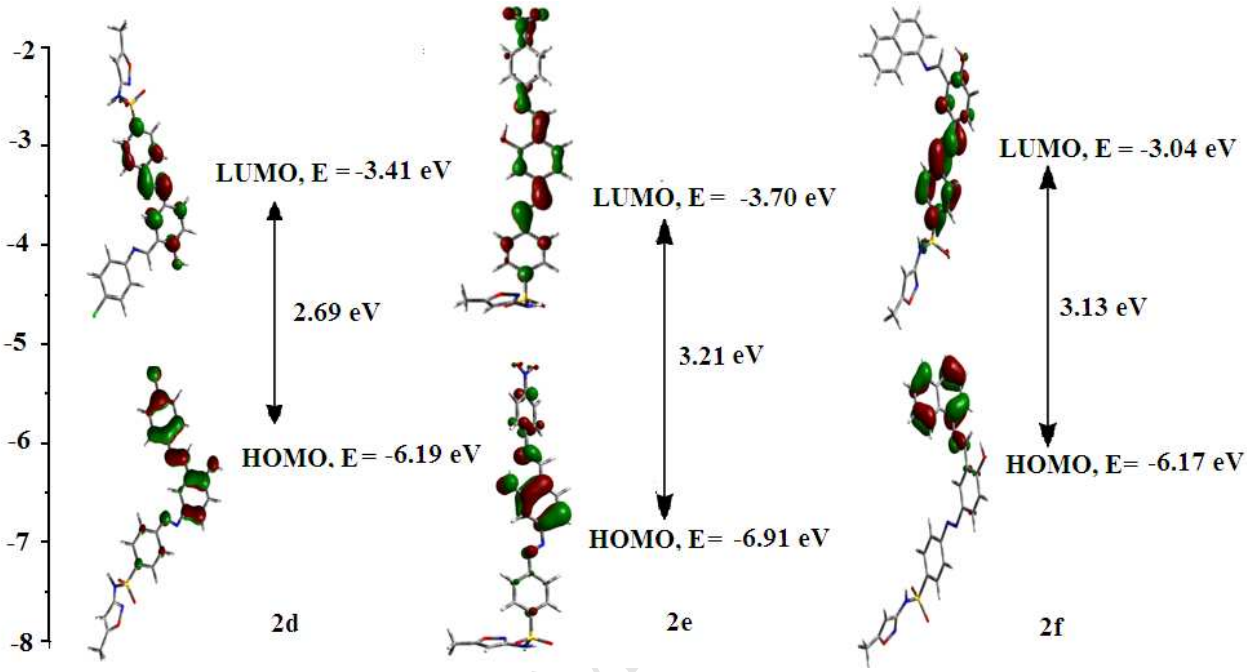

(**c**)

Fig. 12. The HOMO–LUMO energy gap and corelation diagram of **1** and the azo-imine derivatives, **2.**

Conclusion

In Twenty first century discovery of new antibiotic is a challenging task. At present a strategy is the functionalization of formerly useful drugs for the making of less toxic more efficient molecule. Sulfamethoxazole is used to synthesize azo and azo-mine functionalized molecules such as [SMX-N=N-C_6H_3-(*p*-OH)(*m*-CHO)] (**1**) and [SMX-N=N-C_6H_3-(*p*-OH)(*m*-HC=N-Ar)] (**2**) (Ar = –C_6H_5 (**2a**), –C_6H_4-*p*-CH_3 (**2b**), –C_6H_4-*p*-OCH_3 (**2c**), –C_6H_4-*p*-*Cl* (**2d**), –C_6H_4-*p*-NO_2 (**2e**), –$C_{10}H_7$ (**2f**)). The antibacterial properties of the compounds have been evaluated against Gram positive bacteria, *B. subtillis* and Gram negative bacteria, *E. coli*. Cell

line toxicity in Vero cells and anti-viral activity against harpies' virus (HSV-1F ATCC-733) are examined. Data reveal that [SMX-N=N-C_6H_3-(*p*-OH)(*m*-CHO)] (**1**) becomes the most efficient drug against *B. subtillis* and also active against HSV-1F infection. *In silico* Docking has been examined by using DFT optimized and X-ray structures of all these molecules with active site residue of DHPS (dihydropteroate synthetase) protein (downloaded from PDB file) to search the most favored binding mode of the drugs and hence their competitive drug efficiency. The MTT assay represents the toxicity of the products, **1** and **2a**-**f**, are quite less where as the activity against gram +ve bacteria is around 3 times more for **1** derivative and for **2a-f** are also lower than that of SMX.

Acknowledgements

Financial support from University Grants Commission (F.42-333/2013(SR)) and the Council of Scientific and Industrial Research (01(2894)/09/EMR-II), New Delhi are gratefully acknowledged. We acknowledge help from Mr. Nayim Sepay, Senior Research Fellow (SRF), Department of Chemistry, Jadavpur University.

Supporting Information

Crystallographic data for the structure have been deposited to the Cambridge Crystallographic Data center, CCDC No.1557829. These data can be obtained free of charge via http://www.ccdc.cam.ac.uk/conts/retrieving.html, or from the Cambridge Crystallographic Data Centre, 12 Union Road, Cambridge CB2 1EZ, UK; fax: (+44) 1223-336-033; or e-mail: deposit@ccdc.cam.ac.uk

Conflict of Interest

The authors have no conflict of interest to declare.

References

[1] F. Bosch and L. Rosich, The Contributions of Paul Ehrlich to Pharmacology: A Tribute on the Occasion of the Centenary of His Nobel Prize, Pharmacology. 82 (2008) 171–179.

[2] M. Wainwright, J. E. Kristiansen, On the 75th anniversary of Prontosil, Dyes and Pigments. 88 (2011) 231 – 234

[3] H. C. Neu and T. D. Gootz., *Antimicrobial Chemotherapy, Chapter 11 in Medical Microbiology*, 4th edition (Ed. S. Baron), Galveston (TX): University of Texas Medical Branch at Galveston. (1996).

[4] J. Zander, S. Besier, S. Faetke, S. H. Saum, V. Mueller, T. A. Wichelhaus, Intern. J. Antimicrob. Agents. 36 (2010) 562-565.

[5] G. C. Slatore, and A. S. Tilles, Immunol. Allergy Clin. North Am. 24 (2004) 477–490.

[6] C. Choquet-Kastylevsky, T. Vial, and J. Descotes, Curr. Allergy Asthma Rep. 2 (2002) 16–25.

[7] L. S. Walmsley, S. Khorasheh, J. Singer, O. Djurdjev, J. Acquir. Immune. Defic. Syndr. Hum. Retrovirol. 19 (1998) 498-505.

[8] S. N. Lavergne, H. Wang, H. E. Callan, B. K. Park, and D. J. Naisbitt, J. Pharmacol. Exp. Ther. 331 (2009) 372–381.

[9] D. J. Naisbitt, J. Farrell, F. S. Gordon, L. J. Maggs, C. Burkhart, J. W. Pichler, M. Pirmohamed, K. B. Park, Mol. Pharmaco. 62 (2002) 628-637.

[10] P. J. L. Daniels , D. F. Rane , S. W. McCombe , R. T. Testa , J. J. Wright , and T. L. Nagabhushan, *ACS Symposium Series*.125 (1980) 371–392.

[11] W. –T. Ewelina, G. Łukasz, CHEMIK. 66 (2012) 1298-1307.

[12] S.Mondal, S. M. Mandal, T. K. Mondal, C. Sinha, Spectrochim. Acta Part A. 150 (2015) 268-279.

[13] S. Mondal, A. K. Bhanja, D. Ojha, T. K. Mondal, D. Chattopadhyay and C. Sinha, RSC Adv. 5 (2015) 73626–73638.

[14] D. Das, N. Sahu, S. Mondal, S. Roy, P. Dutta, S. Gupta, T. K. Mondal, C. Sinha, Polyhedron, 99 (2015) 77–86.

[15] N. Sahu, D. Das, S. Mondal, S. Roy, P. Dutta, N. Sepay, S. Gupta, E. Lopez-Torres and C. Sinha, New J. Chem. 40 (2016) 5019-5031.

[16] P.Mondal, S. P. Parua, P.Pattanayak, U.Das , S.Chattopadhyay, J. Indian Chem. Soc. 92 (2015) 1949-1955.

[17] A.I. Vogel , A.R. Tatchell, B.S. Furnis , A.J. Hannaford, Vogel's Textbook of Practical Organic Chemistry (5th Edition), Longman. (1996).

[18] Bruker, Program name. Bruker AXS Inc., Madison, Wisconsin, USA. (2001).

[19] R. H. Blessing, Acta Cryst. A. 51 (1995) 33–38.

[20] G. M. Sheldrick, *A short history of SHELX*, Acta Cryst A. 64 (2008) 112-122.

[21] L.J. Farrugia, J. Appl. Cryst, 30 (1997) 565-565.

[22] L. J. Farrugia, J. Appl. Cryst. 32 (1999) 837–838.

[23] H. Mukherjee, D. Ojha, H. S. Chandel, S. Bhattacharyya, T. K. Chatterjee, P. K. Mukherjee, S. Chakraborti, D. Chattopadhyay, Microbiol. Res. 168 (2013) 238–244.

[24] Y. Zhang, P. H. But, E. C. V. Ooi, H. X. Xu, G. D. Delaney, H. S. Lee Spencer, S. F. Lee, Antiviral Res. 75 (2007) 242–249.

[25] P. Bag, D. Chattopadhyay, H. Mukherjee, D. Ojha, N. Mondal, M. Chawla Sarkar, G. Das, S. Chakraborti, Virol J. 9 (2012) 98-109.

[26] H. Cheng, X. He, C. Moore, **Mol. Cell. Biol.** 24 (2004) 2932-2943.

[27] P. J. Hay, W. R. J. Wadt, J. Chem. Phys. 82 (1985) 299-310.

[28] M.J. Frisch, G.W. Trucks, H.B. Schlegel, G.E. Scuseria, M.A. Robb, J.R. Cheeseman, G. Scalmani, V. Barone, B. Mennucci, G.A. Petersson, H. Nakatsuji, M. Caricato, X. Li, H.P. Hratchian, A.F. Izmaylov, J. Bloino, G. Zheng, J.L. Sonnenberg, M. Hada, M. Ehara, K. Toyota, R. Fukuda, J. Hasegawa, M. Ishida, T. Nakajima, Y. Honda, O. Kitao, H. Nakai, T. Vreven, J.A. Montgomery Jr., J.E. Peralta, F. Ogliaro, M. Bearpark, J.J. Heyd, E. Brothers, K.N. Kudin, V.N. Staroverov, R. Kobayashi, J. Normand, K. Raghavachari, A. Rendell, J.C. Burant, S.S. Iyengar, J. Tomasi, M. Cossi, N. Rega, J.M. Millam, M. Klene, J.E. Knox, J.B. Cross, V. Bakken, C. Adamo, J. Jaramillo, R. Gomperts, R.E. Stratmann, O. Yazyev, A.J. Austin, R. Cammi, C. Pomelli, J.W. Ochterski, R.L. Martin, K. Morokuma, V.G. Zakrzewski, G.A. Voth, P. Salvador, J.J. Dannenberg, S. Dapprich, A.D. Daniels, Ö. Farkas, J.B. Foresman, J.V. Ortiz, J. Cioslowski, D.J. Fox, GAUSSIAN 09, Revision D.01, *Gaussian Inc*.,Wallingford, CT. (2009).

[29] A. Frisch, A. B. Nielson, A. J. Holder, *GAUSSVIEW User Manual*, Gaussian Inc, Pittsburgh, PA. (2000).

[30] M.E. Casida, C. Jamorski, K.C. Casida, D.R. Salahub, J. Chem. Phys. 108 (1998) 4439 - 4449.

[31] V. Barone, M. Cossi, J. Phys. Chem. A. 102 (1998) 1995 - 2001.

[32] M. Cossi, V. Barone, J. Chem. Phys. 115 (2001) 4708 - 4717.

[33] M.Cossi, N.Rega, G.Scalmani and V.Barone, J.Comput.Chem. 24 (2003) 669-681.

[34] Discovery Studio 3.5 is a product of Accelrys Inc, San Diego, CA, USA.

[35] C.A. Lipinski; F. Lombardo; B.W. Dominy and P.J. Feeney, Adv. Drug. Del. Rev. 46 (2001) 3–26.

[36] D. F. Veber, S. R. Johnson, H. Y. Cheng, B. R. Smith, K. W. Ward, K. D. Kopple, J. Med. Chem. 45 (2002) 2615–2623.

[37] A.-N. M.A. Alaghaz**,** H. A. Bayoumi**,** Y. A. Ammar**,** S. A. Aldhlmani J. Mol. Struc. 1035 (2013) 383-399

[38] P. K. Ojha, K. Roy, Eur. J. Med. Chem. 45 (2010) 4645-4656.

[39] S. Tabassum, M. Afzal, F. Arjmand, Eur. J. Med. Chem. 74 (2014) 694-702.

Highlights

Spectroscopic characterization, antimicrobial activity and Molecular Docking Study of novel azo-imine functionalized sulphamethoxazoles

Nilima Sahu, Sudipa Mondal , Kaushik Naskar, Ananya Das Mahapatra, Suvroma Gupta, Alexandra M. Z. Slawin , Debprasad Chattopadhyay and Chittaranjan Sinha*

- Schiff base of sulfamethoxazole-azo-salicyladehyde, SMX-N=N-salicylaldehyde
- Spectroscopic characterization
- Antimicrobial activity against *B. subtillis* and *E. coli*
- The anti-viral efficiency against harpies virus (HSV-1F ATCC-733)
- The cell line toxicity (Vero cells)